

MODELING THE DISTRIBUTION OF CHEMICAL OXYGEN DEMAND TO DETERMINE THE OPTIMAL MILL EFFLUENT OUTLET LOCATION

Eddy Rachman Gandanegara, *Harman Ajiwibowo, Andojo Wurjanto

Faculty of Civil and Environmental Engineering, Institut Teknologi Bandung, Indonesia

*Corresponding Author, received: 05 Jan. 2019, Revised: 08 Feb. 2019, Accepted: 21 March 2019

ABSTRACT: This paper aims to evaluate three location alternatives and determine the best one for the water effluent outlet based on the resulting chemical oxygen demand (COD) distribution. A prospective bleached chemi-thermomechanical (BCTM) pulp mill located in Muan River, East Kalimantan Province, Indonesia is taken as a study case. The study involves field measurement and numerical modeling using a Surface-water Modelling System. The measurements cover bathymetry, tidal elevation, current velocity, and water quality survey. Using the data from field measurement and NaoTide, the hydrodynamic model (using the RMA2 module) performs well in the validation of tidal elevation and current velocity. In the water quality model (using the RMA4 module), it is found that by placing the outlet at the downstream of Muan River as in Alternative 1, the least COD average distribution is obtained. Further, Alternative 1 is selected as the best location, resulting in 0.0465 km/m³ average COD annually.

Keywords: Hydro-environmental study, Numerical modeling, Effluent outlet, COD distribution, Muan River.

1. INTRODUCTION

In the past few decades, there has been vast industrial growth throughout the world. Such rapid industrial development may result in a decrease in environmental quality. Due to increasing human needs, the level of pollution in the environment increases. Pollution from industrial development is found in air, water and soil. Water is one of the most important natural resources. Apart from personal usage, water is highly needed in various industries. Pulp and paper mills are two of the main water- and energy-intensive industries, comprising the sixth largest water-polluting sector [1].

Chemical oxygen demand (COD) is an index of the organic content in water. The most common substance oxidized by dissolved oxygen in water is biologically derived organic matter, i.e. dead plant and animal waste [2].

The high COD level linked to pollution could be due to a high rate of organic decomposition resulting from human activities on the watershed. These activities produce sewage and agricultural run-off flowing into the reservoir, and this has a negative impact on water quality [3].

Solichin and Othman applied a Surface-water Modelling System (SMS) to predict the status of the water quality of the Brantas River [4]. The results of the simulations are velocity vector distributions and BOD concentrations along the stream of Brantas River.

Akl, El-Azizy, Azeem and Nasser investigated the circulation of the environmental pattern of El Burullus Lake, a northern coastal lake in the Nile

Delta of Egypt, using SMS 12.1. [5]. They modeled both the hydrodynamic and water quality of the system. The model validation shows a good relationship between the measured and computed values. The hydrodynamic results are successfully used as input to the coupled water quality model.

Ajiwibowo, Ash-Shiddiq and Pratama studied the hydro-environmental condition of Dibawah Lake using SMS to present the distribution of the parameters in the existing condition [6]. The contaminant model result shows that the two rivers had the highest sulfide values. The sedimentation model shows one location with the maximum bed change. From those results, the authors recommend routine dredging to maintain the lake capacity.

Ajiwibowo used SMS to investigate the distribution of four parameters (total suspended sediment (TSS), biochemical oxygen demand (BOD), dissolved oxygen (DO) and phosphate) in Kerinci Lake, Jambi Province, Indonesia [7]. The results show that the Tebing Tinggi River outlet has the biggest yearly bed change. The water quality model shows that the BOD, DO, and phosphate concentrations have significantly bigger discharges from the Merao River outlet than from other rivers.

Ajiwibowo, Ash-Shiddiq and Pratama also investigated the distribution of TSS, BOD, DO and phosphate using SMS in Singkarak Lake, Western Sumatra, Indonesia [8]. The results from the constituent model show that Sumpur and Sumani Rivers have the greatest effect on the water quality of the lake. A 30–40 cm per year change in the waterbed is found at the inlets of both of these rivers.

Apart from SMS, Delft 3D [9] and MIKE [10]–

[13] are widely used to model the environmental distribution parameters of rivers, lakes and other bodies of water.

This paper takes a prospective bleached chemical-thermomechanical (BCTM) pulp mill in the area of Muan River, East Kalimantan, Indonesia as a study case.

Fig. 1 presents the study location. Fig. 1(a) gives the area of interest, covering Riko and Muan River. The BCTM pulp mill is shown in Fig. 1(b) in the upstream of Muan River. Muan River is a tributary of Riko River and ends in Balikpapan Bay, as presented in Fig. 1(c).

The developmental impacts on the change of hydro-environmental conditions at the Muan River site are investigated. The objective of this study is to compare three alternatives of effluent outlet location and determine the best one based on the COD distribution derived from the numerical modeling using SMS.

In the SMS, the location of the water intake is assumed to be fixed. While the effluent outlet

locations are planned in three alternatives, shown as red circles (Fig. 1(b)), which are at the river downstream (Alternative 1), adjacent to the intake site (Alternative 2) and at the river upstream (Alternative 3). The distance from the locations to the effluent treatment plant is 2.2 km, 1.2 km and 1.4 km, respectively.

2. DATA ACQUISITION

Field data acquisitions are conducted to obtain the primary data for the SMS model. These preliminary measurements include bathymetry, tidal elevation, tidal current, and water quality field measurements.

2.1 Bathymetry

A single-beam echosounder is used to measured bed elevation. The surveyed bed elevation is shown in Fig. 1(a), which is applied for modeling the local domain. The water depth may reach 30 and 10

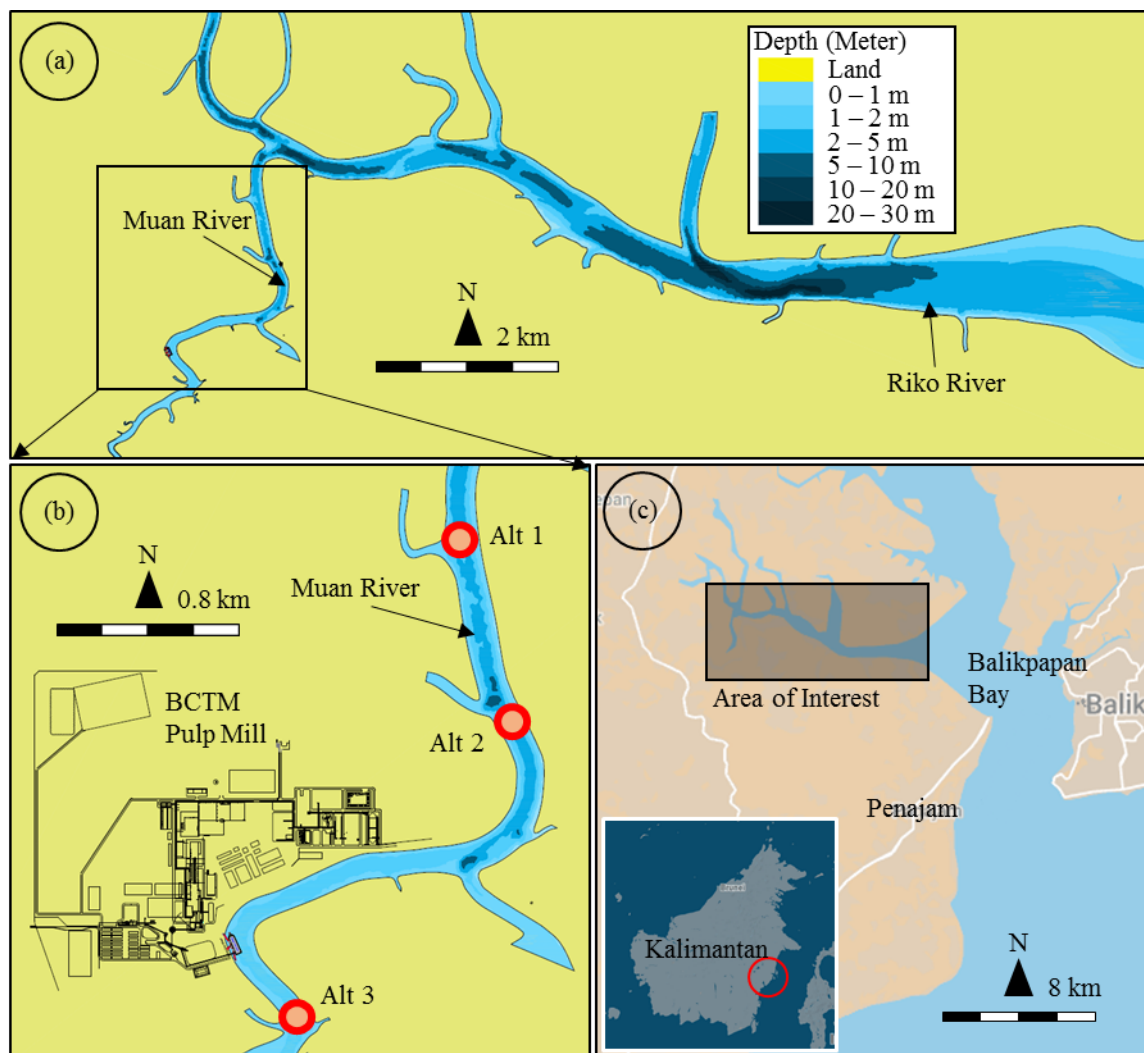


Fig. 1 (a) Bathymetry of Muan and Riko River, (b) Detail view of BCTM Pulp Mill at Muan River, and (c) the location of area of interest

meters in Riko and Muan River, respectively. The global and regional models use secondary data from the Indonesian Navy Navigational Chart.

2.2 Tidal Elevation

The tidal elevation is recorded using a staff-gauge at two locations (TE1 and TE2), as shown in Fig. 2 as black triangles. TE1 and TE2 are in the downstream of Riko River and the upstream of Muan River, respectively.

2.3 Tidal Current

Tidal current measurement is also conducted using the current meter at six locations, depicted as blue triangle markings in Fig. 2. Further, the recorded data will be compared with the model result.

2.4 Water Quality

The water quality measurements consist of in-situ testing and water sampling. The tests are conducted in the middle of nine river cross-sections, shown in Fig. 2 as red triangles. The treated water samples are transported to the Water Quality Laboratory at the Bandung Institute of Technology (Bandung, Indonesia).

The results of the COD laboratory test are presented in Table 1, which shows that COD concentrations from Riko and Muan Rivers exceed the quality standard. According to the Indonesian Government Decree Number 82 (2001) regarding water quality and water pollution control [14], the quality standard for COD concentration from the

nine locations is 47.39 mg/L.

3. NUMERICAL MODEL

The numerical model uses the SMS version 8.1. The SMS is developed by the US Army Corps of Engineers Waterways Experiment Station. The modules for the modeling are the hydrodynamic model (RMA2) and the water quality transport model (RMA4).

3.1 Governing Equations

RMA2 is a two-dimensional depth-averaged finite element hydrodynamic numerical model. It computes water surface elevation and horizontal velocity components for subcritical, free-surface two-dimensional flow fields [15]. Equation (1) is the continuity equation and Eqs. (2) and (3) are the x-direction and y-direction of momentum equations, respectively.

$$\frac{\partial h}{\partial t} + h \left(\frac{\partial u}{\partial x} + \frac{\partial v}{\partial y} \right) + u \frac{\partial h}{\partial x} + v \frac{\partial h}{\partial y} = 0 \quad (1)$$

$$\begin{aligned} h \frac{\partial u}{\partial t} + hu \frac{\partial u}{\partial x} + hv \frac{\partial u}{\partial y} - \frac{h}{\rho} \left[E_{xx} \frac{\partial^2 u}{\partial x^2} + E_{xy} \frac{\partial^2 u}{\partial y^2} \right] \\ + gh \left[\frac{\partial a}{\partial x} + \frac{\partial h}{\partial x} \right] + \frac{gun^2}{\left(1.486h^{1/6} \right)^2} (u^2 + v^2)^{1/2} \\ - \zeta V_a^2 \cos \psi - 2hv\omega \sin \Phi = 0 \end{aligned} \quad (2)$$

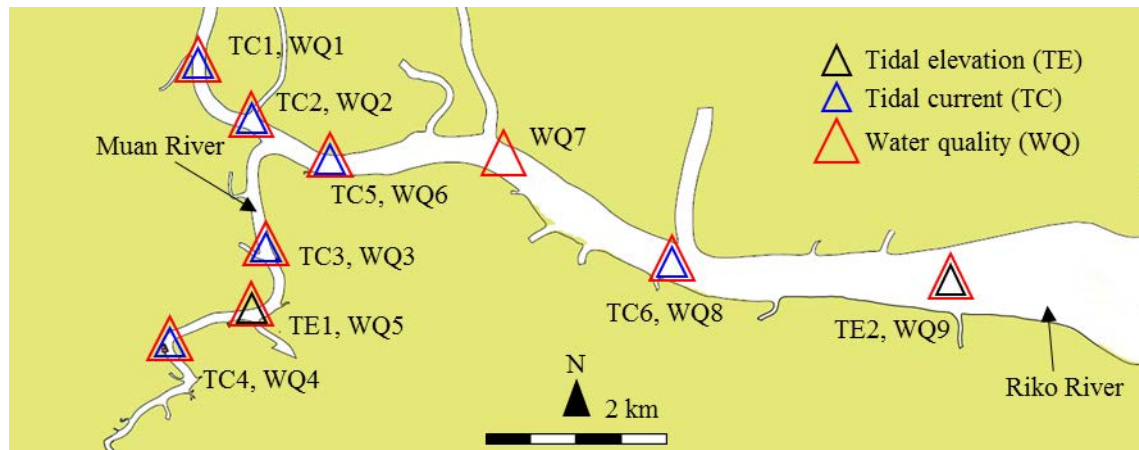


Fig. 2 Locations of tidal elevation, current, and water quality measurements

Table 1 Results of water quality (COD) measurement in 9 locations

River	Muan River			Riko River					
Location (WQ)	4	5	3	1	2	6	7	8	9
COD (mg/L)	52.22	43.52	69.63	43.52	17.41	52.22	78.34	17.41	52.22

$$h \frac{\partial v}{\partial t} + hu \frac{\partial v}{\partial x} + hv \frac{\partial v}{\partial y} - \frac{h}{\rho} \left[E_{yx} \frac{\partial^2 v}{\partial x^2} + E_{yy} \frac{\partial^2 v}{\partial y^2} \right] + gh \left[\frac{\partial a}{\partial y} + \frac{\partial h}{\partial y} \right] + \frac{g v n^2}{\left(1.486 h^{1/6} \right)^2} (u^2 + v^2)^{1/2} - \zeta V_a^2 \sin \psi + 2hu\omega \sin \Phi = 0 \quad (3)$$

where x and y are the Cartesian coordinates, h is the water depth, t is time, u and v are velocities in Cartesian coordinates, E is the eddy viscosity coefficient, ρ is the fluid density, a is the elevation of the bottom, g is the acceleration due to gravity, n is the Manning's roughness n -value, ζ is the empirical wind shear coefficient, V_a is the wind speed, ψ is the wind direction, Φ is the local latitude, ω is the rate of angular rotation of the Earth and 1.486 is the conversion from SI to non-SI units of the momentum equation.

RMA4 is a finite element water quality transport numerical model in which the depth concentration distribution is assumed to be uniform. It computes the concentrations for up to six constituents, either conservative or non-conservative, within a one-and/or two-dimensional computational mesh domain [16].

The water quality model, RMA4, is designed to simulate the depth-average advection-diffusion process in an aquatic environment. The form of the depth-averaged transport equation is:

$$h \left(\frac{\partial c}{\partial t} + u \frac{\partial c}{\partial x} + v \frac{\partial c}{\partial y} - \frac{\partial}{\partial x} D_x - \frac{\partial}{\partial y} D_y - \sigma + kc + \frac{R(c)}{h} \right) \quad (4)$$

where x and y are the Cartesian coordinates, h is the water depth, t is time, u and v are the velocities, c is the concentration of pollutant for a given constituent, t is time, D_x and D_y are turbulent mixing (dispersion) coefficients, k is the first-order decay of pollutant, ρ is the source or sink constituent and $R(c)$ is evaporation/rainfall rate.

3.2 Model Configuration

As presented in Fig. 1(a), the area of interest covers Riko and Muan River. The two rivers are allocated for the local domain. Prior to modelling the local domain, global and regional domains are required to be modeled.

The global model covers Makassar Strait as shown in Fig. 3(a). Fig. 3(b) shows Balikpapan Bay for the regional domain. Fig. 4 shows Muan and Riko Rivers for the local domain. The regional is nested from global domain, and so the local is nested from regional domain. Each of global and regional domains result tidal boundary condition for the regional and local domains respectively. The global model used the NaoTide of Poseidon for tidal constituent at sea boundary [17].

In local model, the forcings for the hydrodynamical process are tidal and river discharges. There are seven tributaries included in local domain. The discharges are given monthly in Fig. 5.

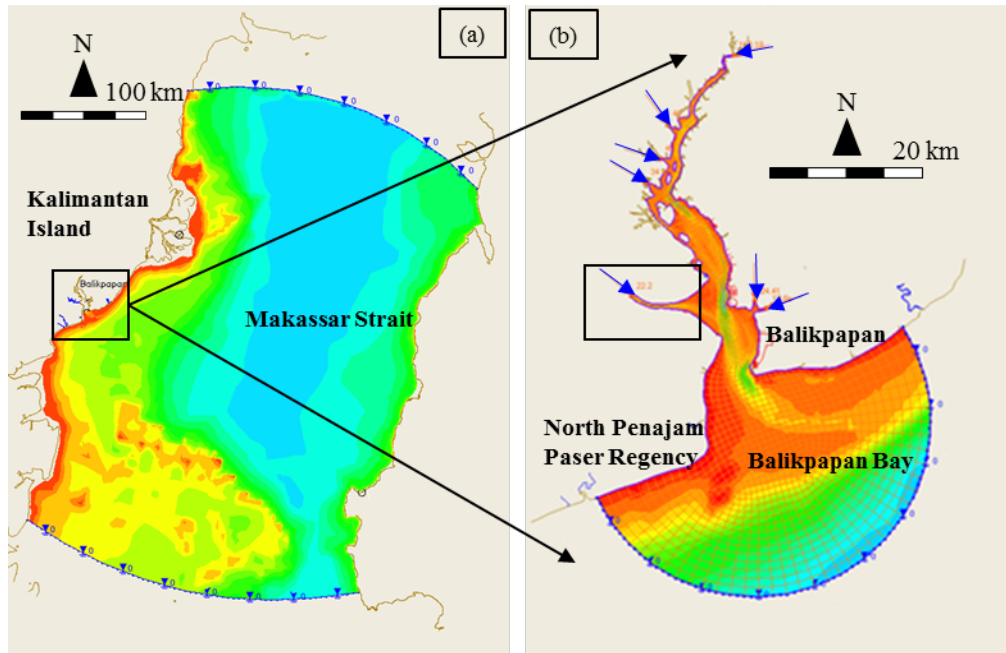


Fig. 3 Overview of (a) global and (b) regional domain. Black box in regional domain shows the coverage of local domain

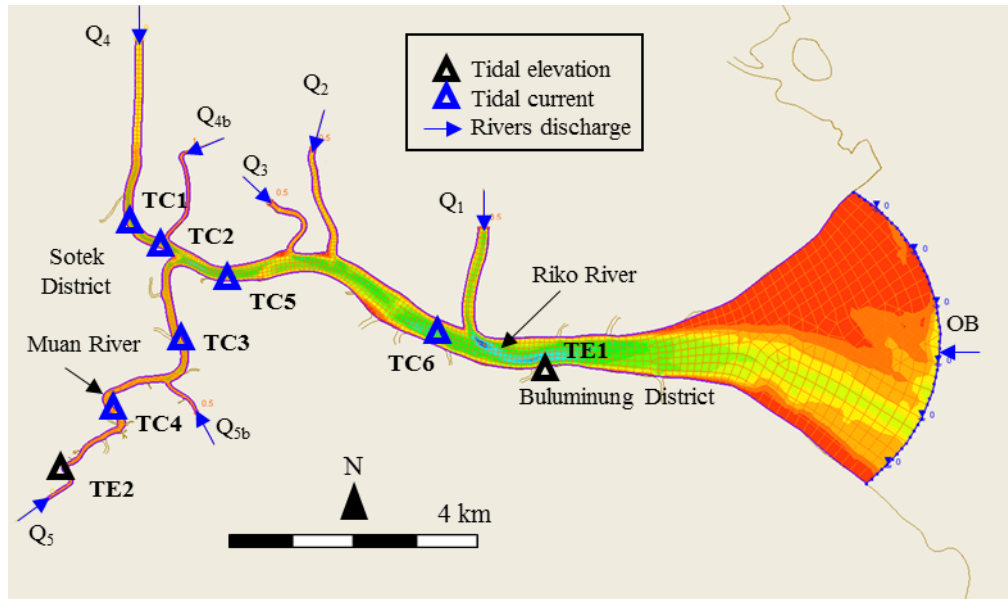


Fig. 4 Mesh and validation location for local domain model

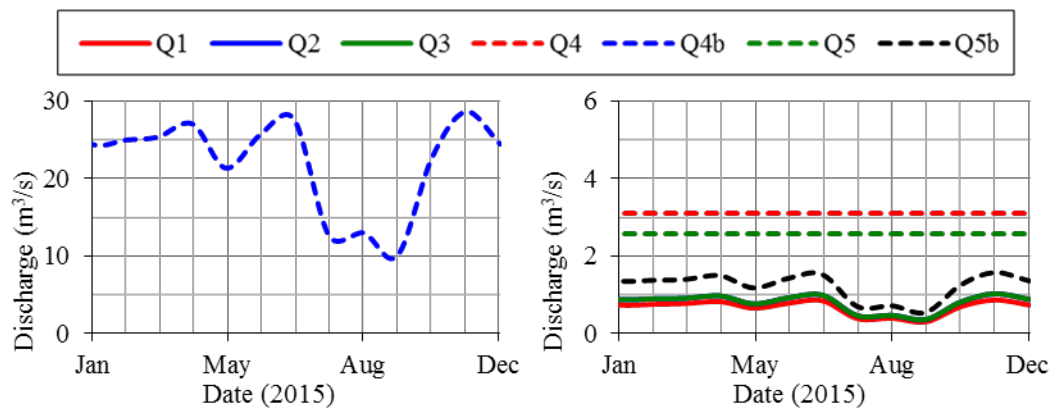


Fig. 5 Discharges of the seven tributaries included in local domain model

Table 2 COD content in boundaries

Boundaries	Notations	COD (kg/m ³)
Water effluent	-	0.3677
Open boundaries	OB	0.0522
River boundaries	Q ₁	0.0174
	Q ₂	0.0783
	Q ₃	0.0783
	Q ₄	0.0435
	Q _{4b}	0.0174
	Q ₅	0.0522
	Q _{5b}	0.0435

At the water intake and outlet, the discharges are 0.2429 and 0.2235 m³/s, respectively [18]. COD

concentrations for open boundaries and effluent outlet are given in Table 2. It is given that the value for effluent outlet is 0.3677 kg/m³ [18].

4. RESULTS AND DISCUSSION

4.1 Model Validation

Tidal elevation validation is conducted for the local domain, and the results are provided in Fig. 6 and Table 3. The validations are conducted at TE1 and TE2, as shown in Fig. 4. The obtained average error is 5.65%.

Using the field current velocity data obtained in six locations (TC1 to TC6) given in Fig. 4, the modeled tidal current is also validated. The validation is presented in a scatter plot in Fig. 7, where the magnitude of modeled and measured data are the x and y-axes, respectively. The comparison shows good results since the dots are scattered near the linear relation (yellow line).

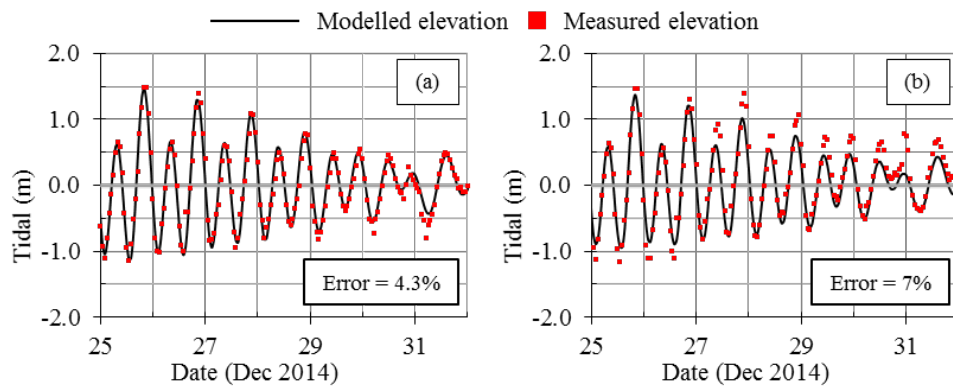


Fig. 6 Results of tidal elevation validation at (a) TE1 and (b) TE2

Table 3 Summary of tidal elevation validation in local domain

Stations	Notations	Duration	Error
River downstream	TE1	Dec 24, 2014 – Jan 8, 2015	4.3%
River upstream	TE2	Dec 25, 2014 – Jan 9, 2015	7%

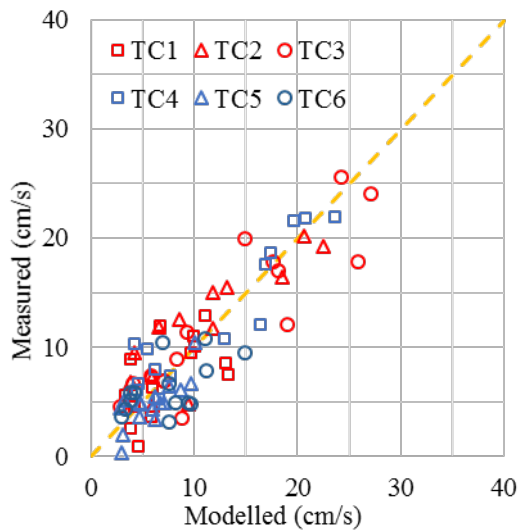


Fig. 7 Scatter plot for tidal current validation

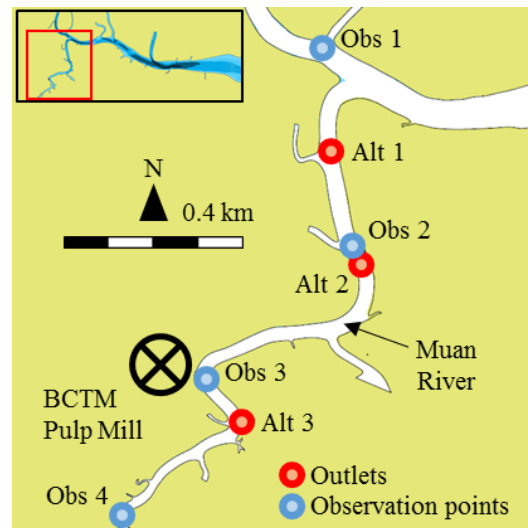


Fig. 8 Locations of alternative outlets and observation points

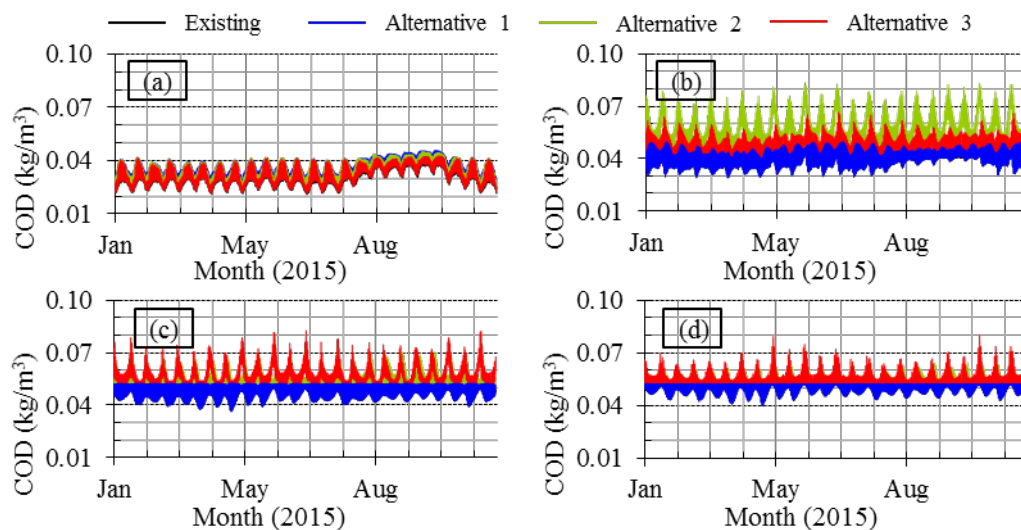


Fig. 9 Results of yearlong COD variation in an existing and three alternative scenarios, each at (a) Obs 1, (b) Obs 2, (c) Obs 3 and (d) Obs 4

Table 4 Summary of yearlong COD variation for all scenarios in four observation points

Location	Value	COD (mg/L)			
		Obs 1	Obs 2	Obs 3	Obs 4
Existing	Max	0.043	0.051	0.053	0.053
	Aver	0.031	0.040	0.051	0.051
	Min	0.021	0.029	0.040	0.040
Alternative 1	Max	0.046	0.059	0.054	0.053
	Aver	0.035	0.048	0.051	0.052
	Min	0.024	0.038	0.044	0.046
Alternative 2	Max	0.045	0.083	0.070	0.064
	Aver	0.035	0.057	0.055	0.053
	Min	0.023	0.036	0.048	0.051
Alternative 3	Max	0.043	0.067	0.083	0.080
	Aver	0.032	0.045	0.056	0.054
	Min	0.021	0.031	0.040	0.046

4.2 COD Distribution

The COD distribution model results are observed at four points, shown in Fig. 8 as blue dots, denoted by Obs 1 to Obs 4. Figs. 9(a) to 9(d) show the one-year simulation model results for each observation location respectively from Obs 1 to Obs 4. Table 4 provides the results of the COD distribution for the existing scenario and Alternatives 1, 2 and 3.

In Table 4, the average of COD concentration for the existing condition and the three alternatives are given. The average COD content of the four observation points in one year for the existing condition is 0.0433 kg/m³. For Alternatives 1, 2 and 3, the average COD concentrations are 0.0465, 0.0500 and 0.0468 kg/m³, respectively. Since Alternative 1 has the smallest value of COD average concentration, it is the most recommended scenario.

5. CONCLUSIONS

A validated model is successfully composed using data from field measurement and NaoTide with three stages of modeling in RMA2. Further, the water quality model in RMA4 shows that Alternative 1 had the best outcome considering that there was the least distribution of COD concentration. The average annual concentration at the four observation points in Alternative 1 is 0.0465 kg/m³.

6. ACKNOWLEDGMENTS

The authors would like to thank the PT. Bukit Muria Jaya Karton for funding this research.

7. REFERENCES

- [1] Kumar V., Dhall P., Naithani S., Kumar A., and Kumar R. Biological Approach for the Treatment of Pulp and Paper Industry Effluent in Sequence Batch Reactor, *Journal of Bioremediation and Biodegradation*, Vol. 5, (3), 2014.
- [2] Gupta P., Vishwakarma M. and Rawtani P.M., Assessment of Water Quality Parameters of Kerwa Dam for Drinking Suitability, *International Journal of Theoretical and Applied Sciences*, Vol. 1 (2), 2009, pp. 53–55.
- [3] Mustapha M.K., Assessment of the Water Quality of Oyun Reservoir, Offa, Nigeria, Using Selected Physico-Chemical Parameters, *Turkish Journal of Fisheries and Aquatic Sciences*, Vol. 8, 2008, pp. 309–319.
- [4] Solichin M. and Othman F., Application of Surface-Water Modelling System (SMS) on River Stream: A Case Study in Brantas River, 4th National Technical Postgraduate Symposium, 2006.
- [5] Akl F., El-Azizy I., Azeem M.A., and Nasser G.A., Environmental Hydrodynamics Mitigation and Water Quality Modelling, Case Study El-Burullus Lake in Egypt Using SMS 12.1, *International Journal of Multidisciplinary Research Review*, Vol. 04 (01), 2017, pp. 2200–2208.
- [6] Ajiwibowo H., Ash-Shiddiq R.H.B., and Pratama M.B., Assessment of Hydro-Environmental Condition Using Numerical

- Modelling in Dibawah Lake, Western Sumatera, Indonesia, *International Journal of GEOMATE*, Vol. 15, Issue 51, 2018, pp. 140–146.
- [7] Ajiwibowo H., Numerical Model of Sedimentation and Water Quality in Kerinci Lake, *International Journal of GEOMATE*, Vol. 15, Issue 51, 2018, pp. 77–84.
- [8] Ajiwibowo H., Ash-Shiddiq R.H.B., and Pratama M.B., Water Quality and Sedimentation Modelling in Singkarak Lake, Western Sumatra, *International Journal of GEOMATE*, Vol. 16, Issue 54, 2019, pp. 94–102.
- [9] Fang H., Huang L., He G., Jiang H., and Wang C., Effects of Internal Loading on Phosphorus Distribution in the Taihu Lake Driven by Wind Waves and Lake Currents. *Environ. Pollut.*, Vol. 219, 2016, pp. 760–773.
- [10] Doulgeris C., Georgiou P., Papadimos D., and Papamichail D., Ecosystem Approach to Water Resources Management using the MIKE 11 Modelling System in the Strymonas River and Lake Kerkini. *J. Environ. Manage.*, Vol. 94, Issue 1, 2012, pp. 132–143.
- [11] Ajiwibowo H., Pratama M.B., Wurjanto A., Assessment of Tidal Current Power Potency in Kelabat Bay, Indonesia, *International Journal of Engineering Technology*, Vol. 9, 2017, pp. 3100–3110.
- [12] Ajiwibowo H., Lodiwa K.S., Pratama M.B., Wurjanto A., Numerical Model of Tidal Current for Power Harvesting in Bangka Strait, *International Journal of Earth Sciences and Engineering*, Vol. 10, 2017, pp. 833–843.
- [13] Ajiwibowo H., Lodiwa K.S., Pratama M.B., Wurjanto A., Field Measurement and Numerical Modeling of Tidal Current in Larantuka Strait for Renewable Energy Utilization, *International Journal of GEOMATE*, Vol. 13, Issue 39, 2017, pp. 124–131.
- [14] Indonesian Government, Indonesian Government Decree Number 82 The Year 2001 Concerning Water Quality and Water Pollution Control, Indonesian Government, 2001.
- [15] User Guide to RMA2 WES Version 4.5. USA: US Army, Engineering Research and Development Center, Waterways Experiment Station, Coastal and Hydraulic Laboratory, 2008, pp. 1–5.
- [16] User Guide to RMA4 WES Version 4.5. USA: US Army, Engineering Research and Development Center, Waterways Experiment Station, Coastal and Hydraulic Laboratory, 2001, Ch. 2, pp. 1–4.
- [17] Matsumoto K, Takanezawa T, Ooe M, Ocean tide models developed by assimilating TOPEX/POSEIDON altimeter data into the hydrodynamical model: a global model and a regional model around Japan, *Journal of Oceanography*, Vol. 56, 2000, pp. 567–581.
- [18] KSH Staff, Pre-feasibility study for BMJ performance board BCTMP and folding boxboard project: Volume 1 – Main report, KSH Consulting, Indonesia, 2013.

Copyright © Int. J. of GEOMATE. All rights reserved, including the making of copies unless permission is obtained from the copyright proprietors.
